Local Ranking of Geostatistical Realizations for Flow Simulation

Jason A. McLennan and Clayton V. Deutsch

Centre for Computational Geostatistics (CCG)
Department of Civil & Environmental Engineering
University of Alberta

Geostatistical reservoir modeling provides multiple equally probable realizations of structure, facies, and petrophysical properties. A large number of realizations should be processed to ensure that production decisions and strategies are not unduly affected by an unusually good or bad simulated realization. Flow simulation, however, often requires significant computational and professional time. Only a few geostatistical realizations can be subjected to detailed flow modeling. An integrated approach is developed for ranking geostatistical realizations. A small number of representative realizations can then be selected for flow processing. The ranking and selecting of realizations must be tailored to the flow process. Techniques that work for conventional oil and gas reservoirs may not be suitable for in-situ and SAGD bitumen recovery methods. This paper describes static connectivity measures increasingly tailored to heavy oil recovery processes from the McMurray Formation. Flow simulation is performed on a number of geostatistical realizations to calibrate the ranking measures to production response. This permits reliable inference in reservoir areas where it is not possible to perform many flow simulations.

Introduction

The Athabasca Oil Sands contained mostly within the McMurray Formation is located northwest of Fort McMurray, Alberta, Canada. The deposit / reservoir is amenable to both surface mining and in-situ recovery methods due to its shallow proximity and high viscosity. At average conditions, there is a 20m net pay interval 120m below the surface with a bitumen viscosity of 10,000,000cp (Komery, 1998). The formation spans 40,000 km^2 and contains an estimated 174.4 billion barrels of bitumen reserves rivaling conventional oil reserves in the Middle East (Polikar, 2004); however, only 10% of the reserves are located close enough to the surface to allow economical surface mining. The demand for innovative in-situ heavy oil sands extraction technology has been on the rise in the last 40 years.

Steam assisted gravity drainage (SAGD) is the most popular thermal in-situ heavy oil recovery process in western Canada. The technology was pioneered and developed by Dr. Roger Butler and his collogues at Imperial Oil in the late 1970's (Butler, 1998). SAGD quickly became a proven technology with successful pilot testing at AOSTRA's Underground Test Facility (UTF) (Komery, 1995). Since the late 1990's, several SAGD projects have been approved with more being planned. Currently, there are over 40 major Oil Sands projects under way or planned with an expected yield of 1.8 million barrels per day by the year 2010 (Moritis, 2004). There are also several foreign SAGD operations and plans such as within the Xinglongtai Formation in the Liaohe Oilfields of China (Shangqi, 1998) and within the Tia Juana field in the Orinoco Belt of Venezuela (Robles, 2001).

Figure 1 illustrates the SAGD concept. The procedure is applied to multiple horizontal well pairs about 1000m long. The upper "injection well" and lower "production well" are nominally parallel and separated by 5m of elevation. To initiate inter-well connectivity, steam is injected through both wells for the first 3 to 6 months. Steam circulation then continues to be injected through the upper injection well only forming a cone shaped steam chamber anchored at the production well. As new reservoir is heated, bitumen lowers in viscosity and flows downward along the outside of the steam chamber boundary via gravity into the production well (Butler, 2004). The primary production performance parameters are the rate oil is produced from the production well (OP_{RATE}) and the amount of steam used relative to oil production or steam-oil-ratio (SOR).

Reservoir geology and heterogeneity certainly affect SAGD production performance (McLennan, 2004). The connectivity of net and non-net reservoir is particularly important. For example, the optimum stratigraphic well pair position that maximizes recovery is directly below significantly thick net sand units (McLennan, 2005). In contrast, low elevation continuous thick shale can result in devastatingly poor production. Although there are many factors that affect SAGD production performance prediction, connectivity and the spatial distribution of facies, porosity, water saturation, and permeability are the most significant.

Geological heterogeneity and connectivity is impossible to exactly predict between wells. The unique true distribution of reservoir properties will remain unknown. Geological uncertainty is an inherent characteristic of any geological model. Geostatistics can be used to quantify uncertainty in the geological model through the construction of multiple equally probable realizations of reservoir properties. The difference between geological realizations is a measure of geological uncertainty (Deutsch, 2002a).

The main objective of using geostatistics to characterize a potential SAGD reservoir is to quantify the uncertainty in production performance (OP_{RATE} and SOR) due to geological uncertainty. Figure 2 illustrates this concept schematically. Flow modeling is a transfer function converting the geological uncertainty to production uncertainty, that is, for each geological realization, flow simulation provides the corresponding OP_{RATE} and SOR response. The difference between production parameter realizations is a measure of production uncertainty.

The required level of geological detail and complex heat transfer equations make simulating SAGD flow on a large number of detailed geological realizations impossible. Consider in Figure 3 a phase of SAGD operations where 40 well pairs stemming from 4 drilling pads are needed to fully sweep the net reservoir within 4 sections of a township lease. Assume 100 high resolution geological realizations are required to fully characterize the geological uncertainty within each of the 52 cumulative steam chamber volumes. A total of 4,000 geological realizations then need to be processed through the flow simulator to characterize production uncertainty. This is clearly intractable – the geological input to flow simulation must be reduced.

Ranking

A group of techniques collectively referred to as *ranking* allows flow modeling only a few geological realizations to represent production uncertainty fairly. Randomly choosing a limited number of geological realizations will not accurately represent uncertainty; ranking is a superior method that selects expected and bounding flow response cases that accurately represent production uncertainty (Deutsch, 1996). Ranking is an especially important preliminary step

before SAGD flow characterization since there are usually both multiple geological realizations and multiple drainage volumes to consider.

The idea of ranking geostatistical realizations was popularized in geostatistics in 1992 (Ballin, 1992). The central goal of ranking is to exploit the simplest geological measure possible to accurately select the *low* (p10), *medium* (p50) and *high* (p90) geological realizations that correspond to the *low* (p10), *medium* (p50) and *high* (p90) production responses. The flow results from these few geological realizations will then effectively characterize production uncertainty by distinguishing the expected and bounding flow behavior.

In order for the selection of geological realizations to be accurate, the ranking measure must be highly correlated to production performance. To achieve suitably high correlations, the subsequent recovery process should be accounted for or integrated into the ranking parameter calculation methodology. The correlation between the ranking parameter and production performance is the central criteria used to evaluate the effectiveness of the ranking process. This correlation often increases with increasing customization to the flow process.

Figure 4 illustrates a simple ranking measure within a typical McMurray Formation SAGD reservoir. A total of 101 geological realizations are built within each of 4 well pair drainage volumes. Volume of sand is chosen as the ranking measure and calculated for each suite of realizations. From each drainage volume, the geological realization corresponding to the lowest, medium, and highest sand volume are selected for flow processing. The 12 solid black points show excellent correlation between the ranking measure and OP_{RATE} and SOR production performance variables. This correlation can then be filled in (shaded points) so that the production response for any sand volume at future well pair location can be predicted without running additional flow simulations.

A good ranking is achieved when the measure is tailored to the flow process. This framework has resulted in a variety of ranking methodologies and measures throughout the petroleum industry. The measures can be grouped into 2 general categories:

1. *Static* geological measures employing statistical calculations of such as connectivity, conductivity, and tortuosity.
2. *Dynamic* flow simulation approximations employing quick flow-physics setups such as random-walk, time-of-flight (TOF), tracer, or streamline setups.

Dynamic ranking measures and methodologies have received significant attention in the past 10 years. Indeed, it is tempting to use such fit-for-purpose measures for ranking; however, there are a number of disadvantages. Most importantly, dynamic ranking measures tend to exceedingly depend on the simplifying flow-physics approximations rather than the underlying geological heterogeneity and uncertainty (Gilman, 2005). This phenomenon can manifest in difficulties correlating the ranking measure to production response. Often, in order to obtain acceptably high correlations, many simplifying assumptions need to be withdrawn and accounted for which increases the computational effort towards that of full flow modeling (Saad, 1996). Moreover, several evolving production constraints such as well placement and injection and production controls can be cumbersome to incorporate into a dynamic ranking methodology (Ates, 2005). Although dynamic ranking certainly accounts for the production mechanism, these measures are not simple and tend to undermine the geological uncertainty through its simplifying assumptions.

Static ranking measures are straightforward. They and can be easily calibrated to SAGD production performance response with high correlation (Deutsch, 2002b). This paper describes

static connectivity measures increasingly tailored to heavy oil recovery processes from the McMurray Formation. Flow simulation is performed on many geostatistical realizations to calibrate the ranking measures to production response. The ranking measures are then evaluated and interpreted on the basis of their relative correlation to OP_{RATE} and SOR performance.

Some effort is required to customize the calculation of static ranking measures to SAGD production performance. The procedures and calculations must somehow account for the dynamics of SAGD flow without numerically solving complex fluid flow equations. This is done by calculating measures of connectivity. The response from virtually any SAGD reservoir heterogeneity can be well correlated to measures of connectivity.

Connectivity

Ranking geostatistical realizations for SAGD performance prediction is a relatively new and unique process. Conventional volumetric ranking measures such as original-oil-in-place (OOIP) may not be acceptable. Statistical ranking measures are equally ineffective. The SAGD process depends on the efficient connection of the steam chamber to the surrounding reservoir; therefore, the ranking measures must somehow account for connectivity. Conventional global connectivity calculations would indicate the proportion of net reservoir that is connected within the drainage volume; however, these procedures will only correlate well in relatively homogeneous reservoirs. For heterogeneous reservoirs typical of the McMurray Formation with significant impermeable shale units, local connectivity must be considered.

Local connectivity is defined as either the success or failure of the steam chamber to reach and recover bitumen within local windows of an expected SAGD drainage volume. Consider 3 such local windows superimposed on a long section through a SAGD drainage volume in Figure 5. The facies model and well trajectory are indicated; non-net reservoir is interpreted as shale. The behavior of the steam chamber in each window will be different. In the left window, steam will connect to the entire net reservoir. Steam will also connect to the entire net reservoir in the middle window; however, marginal shale edges make its path more burdensome. On the right, a thick shale unit drapes over the entire local window at a very low depth; here, steam will not reach the *net* reservoir above the shale. This reservoir will be incorrectly characterized as producible by a global connectivity calculation. A local connectivity calculation is needed to discount such net reservoir units that cannot be produced by the SAGD mechanism. The bottom of the figure illustrates the results of a local connectivity calculation within the three windows.

Local connectivity is the most complex ranking measure considered in this work. Relative to conventional OOIP, statistical, and global connectivity calculations, measures of discounted or local connectivity are superior predictors of OP_{RATE} and SOR production. We now formulate and describe the ranking measures used in this work.

Ranking Measures

Several ranking measures are formulated in this work. There are 4 different classes of static ranking procedures: (1) volumetric, (2) statistical, (3) global connectivity, and (4) local connectivity. There are 2 different ranking measures considered in the volumetric, global connectivity, and local connectivity methods and 3 different ranking measures considered in the statistical methods making 9 separate ranking measures in total. We assume that multiple 3D geostatistical realizations of facies, porosity, water saturation, and permeability are available.

Volumetric. Volumetric type calculations are the simplest ranking measures. Original-oil-in-place $OOIP^l$ is calculated on each realization l from l =1,..,L as:

$$OOIP^l = \sum_{z=1}^{Z}\sum_{y=1}^{Y}\sum_{x=1}^{X} V_{(x,y,z)} \cdot \left(1 - S^l{}_{(x,y,z)}\right) \cdot \phi^l_{(x,y,z)} \tag{1}$$

where X, Y, Z are the number of cells in the east, north, and elevation directions; x, y, z indicates a 3D cell location; V is the volume of each cell; ϕ is the porosity; and S is the water saturation. An improvement on the $OOIP^l$ calculation is a net oil-in-place $OIP^l{}_{NET}$ calculation where only those cells satisfying some combination of facies, porosity, and permeability cutoff criteria are included in the sum:

$$OIP^l_{NET} = \sum_{z=1}^{Z}\sum_{y=1}^{Y}\sum_{x=1}^{X} V_{(x,y,z)} \cdot \left(1 - S^l{}_{(x,y,z)}\right) \cdot \phi^l_{(x,y,z)} \cdot i^l_{NET(x,y,z)} \tag{2}$$

where the indicator transform $i^l{}_{NET}$ defines the net cutoff criteria:

$$i^l_{NET(x,y,z)} = \begin{cases} 1, \ if \quad fcs^l_{(x,y,z)} = netfcs_p \ ; and \\ \qquad \phi^l_{(x,y,z)} > \phi_C \ ; and \\ \qquad k^l_{(x,y,z)} > k_C \\ 0, \ otherwise \end{cases} \qquad p = 1,..,P \tag{3}$$

where k is the permeability, fcs is the facies code and $netfcs_p$, p = 1,..,P are the net facies codes and ϕ_C and k_C are porosity and permeability cutoffs. Any cell within the reservoir that is non-net ($i^l{}_{NET}$ = 0) has either a non-net facies type, ϕ lower than ϕ_C, or k lower than k_C and is not included in the OIP_{NET} calculation.

Statistical. Statistical ranking measures are also very simple. For this work, the average porosity, water saturation, and permeability are used as ranking measures. They are calculated as:

$$\phi^l_{AVG} = \frac{\sum_{z=1}^{Z}\sum_{y=1}^{Y}\sum_{x=1}^{X} \phi^l_{(x,y,z)}}{XYZ}; S^l_{AVG} = \frac{\sum_{z=1}^{Z}\sum_{y=1}^{Y}\sum_{x=1}^{X} S^l_{(x,y,z)}}{XYZ}; k^l_{AVG} = \frac{\sum_{z=1}^{Z}\sum_{y=1}^{Y}\sum_{x=1}^{X} k^l_{(x,y,z)}}{XYZ} \tag{4}$$

Arithmetic averages are implemented. Although permeability does not average arithmetically, simple averaging processes are rank preserving. Average facies types could also be calculated. Ranking can be based on net sand proportion as in Figure 4 or based on non-net shale proportion.

Global Connectivity. Global connectivity is an important indicator of SAGD production performance. While global connectivity calculations are more difficult than volumetric and statistical type static measures, they are less complex than local connectivity calculations.

A cell is deemed globally connected when it is net ($i^l{}_{NET}$ = 1) and connected to one or more neighboring net cells. Here, being *connected* requires the net cell shares either coincidental faces, corners or edges with another net reservoir cell. A global connectivity indicator is defined as:

$$i^{(l)}_{GC}(x,y,z) = \begin{cases} 1, \ if \ connected \\ 0, \ if \ unconnected \end{cases} \tag{5}$$

This is a more strict approach than the $i^l{}_{NET}$ indicator alone, that is, some reservoir cells that are net reservoir are not connected ($i^l{}_{NET}$ = 1; $i^l{}_{GC}$ = 0). However, global connectivity measures are an

improved predictor of SAGD production performance. The fraction of globally connected cells can be calculated as:

$$F_{GC}^{l} = \frac{\sum_{z=1}^{Z}\sum_{y=1}^{Y}\sum_{x=1}^{X} i_{NET(x,y,z)}^{l} \cdot i_{GC(x,y,z)}^{l}}{XYZ} \tag{6}$$

Only cells that satisfy the net reservoir criteria and are connected to other net reservoir cells are included in this fraction. Multiple groups of globally connected cells or geo-objects can exist in any single geological realization. The F_{GC} measure considers all geo-objects within each realization. Conventional global connectivity ranking measures are often based on statistical measures considering only the first N largest geo-objects. N is usually between 1 and 10. For example, average tortuosity T can be calculated as:

$$T^{l} = \frac{\sum_{n}^{N} \frac{SA_n}{V_n}}{N} \tag{7}$$

where SA and V are the surface area and volume of the n^{th} geo-object. The idea is that those realizations that contain geo-objects with high tortuosity, that is, relatively large surface area to volume ratios, are good indications of poor SAGD production performance.

Local Connectivity. Local connectivity is an excellent indication of OP_{RATE} and SOR. Although local connectivity is the most complex static ranking measure considered in this work, they should correlate the best to SAGD production performance. Moreover, these measures are more straightforward than solving the complex fluid flow equations involved in dynamic type ranking measures. The calculation of local connectivity measures for ranking realizations is still relatively new in practice and in the literature. Similar to global connectivity, the local connectivity program acts as an indicator transform:

$$i_{LC}^{(l)}(x,y,z) = \begin{cases} 1, & \textit{if connected} \\ 0, & \textit{if unconnected} \end{cases} \tag{8}$$

A cell is locally connected when it itself is net ($i_{NET}^{l} = 1$) and is connected to net cells either directly above or below within the same aerial stack of cells. Here, being *connected* requires implementing the local connectivity program for which there are a number of details to clarify.

Consider the series of examples in Figures 6 through 8. SAGD injector-producer well pairs are shown as dots and net and non-net reservoir cells are represented by yellow and black, respectively. Conventional global connectivity calculations would essentially consider the entire reservoir as one connected geo-object since the fraction of net cells is large. This is problematic since the non-net reservoir (shale) effectively isolates the upper *net* reservoir. The local connectivity program works within local columns of reservoir cells defined by X and Y window sizes. Figure 7 limits the connectivity calculation to 3 grid cells; here, only 4 cells are deemed connected within the column above the SAGD well pair. The connectivity for a particular column of cells only includes those cells in the same column – even if they must be connected through other cells within the window tolerance. The column of 7 cells in Figure 8 is connected since they are connected within the window tolerance. The aerial location for connectivity calculation is scanned over the entire reservoir to yield connectivity calculations for each stack of cells.

The elevation of the first cell considered in calculating connectivity within a particular stack of cells is important. There may be a number of isolated connected zones. Figure 9 shows seven isolated intervals of thickness 1, 5, 2, 1, 4, 1, and 1 from top to bottom. It would be inappropriate to start the connectivity calculation within the upper thickness 5. In practice, only one could be produced by SAGD production. Specifically, the lower reservoir will be produced where the well pair is located with an expectation to connect some of the upper material. The lower reservoir zones should be preferred. This is done by weighting each string of connected cells according to the linear function shown in red and bold arrowheads. The interval with the highest weighted-thickness is chosen as the initial interval for connectivity calculation.

There are a number of outputs from the local connectivity calculation program. The outputs used for this work are the 3D connectivity indicator i^l_{LC} and the 2D connected thickness. The fraction of locally connected cells is used as a local connectivity ranking measure:

$$F^l_{LC} = \frac{\sum_{z=1}^{Z}\sum_{y=1}^{Y}\sum_{x=1}^{X} i^l_{NET(x,y,z)} \cdot i^l_{LC(x,y,z)}}{XYZ} \tag{9}$$

This is a more strict approach than the i^l_{GC} indicator, that is, some reservoir cells that are net reservoir and globally connected are not locally connected ($i^l_{NET} = 1$; $i^l_{GC} = 1$; $i^l_{LC} = 0$). A more complete formula for the F_{LC} measure represents this series of increasingly complex ranking measures:

$$F^l_{LC} = \frac{\sum_{z=1}^{Z}\sum_{y=1}^{Y}\sum_{x=1}^{X} i^l_{NET(x,y,z)} \cdot i^l_{GC(x,y,z)} \cdot i^l_{LC(x,y,z)}}{XYZ} \tag{10}$$

There are some sensitive parameters involved in defining the local connectivity calculations such as the definition of the net reservoir indicator i^l_{NET}, the window tolerances, and the form of the weighting function. Different values for these parameters will correlate differently to SAGD production. This implies there is an optimal set of parameters for ranking realizations. The optimal window size in the *Y* direction is considered in this work.

Example Setup

A suite of 100 geological realizations of facies, porosity, water saturation, and permeability are constructed within a single SAGD drainage volume using geostatistical simulation. The realizations are synthetically created with the intention of mimicking a high quality net pay McMurray Formation interval. Uncertainty in the top and bottom surfaces is not considered. There are 5 facies types: sand, breccia, interbedded sand, interbedded shale, and shale. The porosity, water saturation, and permeability variables are modeled separately within each facies. Two horizontal strings of data coincident with the subsequent well pair trajectory are used to condition the simulation of each variable.

Figure 10 shows a central *XY* (left), *XZ* (middle), and *YZ* (right) cross sectional view through the 50th of 100 geological realizations. For simplicity, the realizations are constructed at the support of the intended flow simulation grid. To decrease the flow simulation run times, there are 16 x 75 x 50 grid cells (60,000 total) measuring 50m x 2m x 2m in the *X*, *Y*, and *Z* directions, respectively, for a total of 60,000 cells per realization.

Flow simulation is performed to calibrate the subsequent ranking measures. A single 500m long well pair is used. The production and injection well are located 19 and 25m from the base of the reservoir, respectively. The project life is 6.5 years including a 6 month hot finger stimulation startup, a 2 year high pressure phase, a 2 year low pressure phase, and a 2 year blowdown phase. The flow simulations produce the OP_{RATE} and SOR response. The cumulative OP_{RATE} and SOR at the end of the blowdown phase are used to calibrate the ranking measures.

A total of 20 geological realizations are selected for flow processing. The simplest ranking measure *OOIP* is calculated for all 100 realizations and then the P03, P08, P13,…, P98 realizations are chosen for flow modeling. Table 1 shows the *OOIP* ranking results including the realization number, rank out of 100, rank out of 20 cumulative SOR, cumulative SOR rank out of 20, cumulative OP_{RATE}, and cumulative OP_{RATE} rank out of 20. Figure 11 shows the OP_{RATE} and SOR profiles as well as the steam chamber shape (100^0C iso-surface) during the high pressure phase of the 10^{th} ranked (relative to SOR) realization.

The ranking measures previously formulated are now calculated on all 100 realizations and on the 20 realizations selected for flow modeling. The net indicator i_{NET} is defined by $netfcs_p$, p = 1 (sand), 2 (breccia), 3 (interbedded sand), ϕ_C = 0.25, and k_C = 100mD. N = 3 geo-objects are considered for the global tortuosity ranking. An X and Y window size of 0 and 1 are used. This corresponds to calculating local connectivity within 6m in the Y direction and 50m in the X direction. The ranking measure results are presented for all 100 realizations and for the 20 realizations selected for flow simulation separately.

Figures 12 through 15 show the volumetric, statistical, global connectivity, and local connectivity ranking measure results for all 100 realizations. For each ranking measure a frequency and cumulative histogram are shown. Tables 2 through 5 show the volumetric, statistical, global connectivity, and local connectivity ranking measure results for the realizations selected for flow processing. These tables report the value of the ranking measure and its resulting rank out of 20. The correlation between each of the ranking measures and the cumulative OP_{RATE} and SOR production performance response variables is shown in Table 6. The local ranking calculation is then repeated for Y window sizes of 2, 5, 10, 15, and 20 cell radii. The ranking results for these cases are summarized by their correlation to SAGD production performance in Table 7.

Table 1 shows that *OOIP* is not a good predictor of SAGD production performance. Only the 18^{th} ranked realization (realization 31 out of 100) is correctly ranked. Table 2 shows both the *OOIP* and OIP_{NET} ranking results. Table 6 shows that neither of the 2 volumetric ranking measures correlate well to either OP_{RATE} or SOR. The statistical ranking measures ϕ_{AVG}, S_{AVG}, and k_{AVG} in Table 3 are even worse in their ability to identify the ranked production performance. Their correlations in Table 6 are lower than those for the volumetric measures. In contrast, the global connectivity ranking measures F_{GC} and T in Table 4 perform quite well with correlations on the order of +/- 0.9. Local connectivity performs the best, see Tables 5 and 6. Both the F_{LC} and *THK* measures correctly rank each of the 20 geological realizations in terms of cumulative SOR. The resulting correlation is nearly 1.0. The cumulative OP_{RATE} calibrates slightly worse to the local measures with correlations around 0.9. Finally, the Y window tolerance sensitivity study indicates that the 5 cell radius is optimal.

Discussion on Ranking for Example

The previous implementation illustrated the relative effectiveness of 9 different static ranking measures for a potential SAGD reservoir. Static measures of local connectivity were the most

effective since their correlation to OP_{RATE} and SOR were the highest. This means that, more than any other ranking measure, local connectivity will most accurately identify the geological realizations corresponding to low, medium, and high OP_{RATE} and SOR responses.

Once the most appropriate ranking measure is selected, the methodology for ranking and selecting geostatistical realizations for flow processing is simple. The ranking measure is calculated for every geostatistical realization. Within every drainage volume of interest, the *low* (p10), *medium* (p50) and *high* (p90) geological realizations are then selected for flow modeling. If the correlation to OP_{RATE} and SOR is excellent, these selected realizations will produce the corresponding *low* (p10), *medium* (p50) and *high* (p90) production realizations.

Conclusion

The reservoir created for this work is of very high quality with a small fraction of non-net material; therefore, global connectivity satisfactorily predicts SAGD production performance with correlations of around 0.9. Nevertheless, local connectivity is still an important consideration in order to identify each realization correctly.

Many other static ranking measures exist. The ones chosen in this report are intended to be representative of industry practice. Ranking by measures of local connectivity is relatively new and undocumented; however, the professional time required implementing local connectivity calculations is worth the improved ability to correctly identify the bounding geological uncertainty that corresponds to the bounding production uncertainty after flow processing.

This paper does not address many sources of geological uncertainty. Other than the geological heterogeneity, the volume support or scale difference between core measurements and geological modeling cells, the limited flexibility of our geostatistical modeling techniques to reproduce complex non-linear spatial features, numerical error from the approximate solution of non-linear partial differential equations, error from the 3-phase approximation of Darcy's Law all contribute to uncertainty in the transfer of geological uncertainty to production uncertainty.

We have not restricted ourselves further than just plausible realizations. For example, there are times when it is appropriate to discard geostatistical realizations on the basis of simply visual inspection or data such as seismic not used in the geostatistical modeling; however, we consider all realizations that meet some minimum acceptance criteria. For this paper, this criterion is the data being honored at their locations, the input histogram being honored, and the input spatial correlation being honored.

Dynamic ranking measures suffer from strong simplifying assumptions that mask geological heterogeneity. Static ranking measures explicitly account for geological heterogeneity modeled by geostatistics. By considering local connectivity, static ranking measures can be easily correlated to OP_{RATE} and SOR response variables. This allows the reliable selection of bounding production performance uncertainty.

References

1. Komery, D., Luhning, R. and Pearce, J., 1998. *Pilot Testing of Post-Steam Bitumen Recovery from Mature SAGD Wells in Canada*, Canadian Institute of Mining and Metallurgy (CIM), no. 214.
2. Polikar, M., 2004. *Thermal Recovery*, Edmonton: University of Alberta. [Course notes.]

3. Deutsch, C., Dembicki, E. and Yeung, K., 2002. *Geostatistical Determination of Production Uncertainty: Application to Firebag Project*, Center for Computational Geostatistics (CCG), University of Alberta, Edmonton, Alberta, Canada.

4. Butler, R., 1998. *SAGD Comes of AGE!*, Journal of Canadian Petroleum Technology, 37(7):9-12.

5. Komery, D., Luhning, R. and O'Rourke, 1995. *New Era for Oil Sands Development – SAGD Project*, 6th UNITAR International Conference on Heavy Crude and Oil Sands, Houston, USA, February, 1995.

6. Moritis, G., 2004. *Oil Sands Drive Canada's Production Growth*, Oil and Gas Journal, June 7, 2004.

7. Shangqi, L., Yongrong, G., Zhimian, H., Naiqun, Y., Liping, Z. and Suning, H., 1998. *Study on Steam Assisted Gravity Drainage with Horizontal Wells for Super-Heavy Crude Reservoir*, Canadian Institute of Mining and Metallurgy (CIM), no. 217.

8. Robles, J., 2001. *Application of Advanced Heavy-Oil-Production Technologies in the Orinoco Heavy-Oil-Belt, Venezuela*, Society of Petroleum Engineers (SPE), Paper no. 69848.

9. Butler, R., 2004. *Thermal Recovery of Oil and Bitumen*, GravDrain Inc., Calgary, Alberta, 1997.

10. McLennan, J. and Deutsch, C, 2004. *SAGD Reservoir Characterization Using Geostatistics: Application to the Athabasca Oil Sands, Alberta, Canada*, Center for Computational Geostatistics (CCG), September, 2004.

11. McLennan, J., Ren, W., Leuangthong, O. and Deutsch, C., 2005. *SAGD Well Optimization*, AAPG Annual Conference, June, 2005.

12. Deutsch, C., Dembicki, E. and Yeung, K., 2002a. *Geostatistical Determination of Production Uncertainty: Application to Firebag Project*, Center for Computational Geostatistics (CCG), University of Alberta, Edmonton, Alberta, Canada.

13. Deutsch, C. and Srinivasan, S., 1996. *Improved Reservoir Management through Ranking Stochastic Reservoir Models*, Society of Petroleum Engineers (SPE), Paper no. 35411.

14. Deutsch, C. *Geostatistical Reservoir Modeling*. Oxford University Press, 2002b.

15. Ballin, P., Journel, A. and Aziz, K., 1992. *Prediction of Uncertainty in Reservoir Performance Forecasting*, Journal of Canadian Petroleum Technology (JCPT), no.4, April 1992.

16. Gilman, J., Meng, H., Uland, M., Dzurman, P. and Cosic, S., 2005. *Statistical Ranking of Stochastic Geomodels Using Streamline Simulation: A Field Application*, Society of Petroleum Engineers (SPE), Paper no. 77374.

17. Saad, N., Maroongroge, V. and Kalkomery, C., 1996. *Ranking Geostatistical Models Using Tracer Production Data*, Society of Petroleum Engineers (SPE), Paper no. 35494.

18. Ates, H., Bahar, A., El-Abd, S., Charfeddine, M., Kelkar, M. and Datta-Gupta, A., 2005. *Ranking and Upscaling of Geostatistical Reservoir Models by use of Streamline Simulation: A Field Case Study*, SPE Reservoir Evaluation and Engineering, February, 2005.

FLOW SIMULATION RESULTS								
NUMBER	REALIZATION	OOIP			SAGD PRODUCTION			
		RANK (100)	RANK (20)	*OOIP* (x10^6)	SOR (m^3/m^3)	SOR RANK	O_{RATE} (x10^{6}m^3)	O_{RATE} RANK
1	50	3	1	2.298	1.811	3	0.325	11
2	59	8	2	2.415	1.718	5	0.311	8
3	88	13	3	2.436	1.898	2	0.243	2
4	2	18	4	2.455	1.707	6	0.294	5
5	37	23	5	2.478	1.676	7	0.305	7
6	3	28	6	2.520	1.604	11	0.336	13
7	56	33	7	2.540	1.611	10	0.290	4
8	60	38	8	2.568	1.527	15	0.339	14
9	23	43	9	2.579	1.600	12	0.328	12
10	40	48	10	2.596	1.520	16	0.360	15
11	64	53	11	2.623	1.595	13	0.318	10
12	95	58	12	2.637	1.670	8	0.295	6
13	86	63	13	2.646	1.911	1	0.214	1
14	81	68	14	2.663	1.461	17	0.382	17
15	42	73	15	2.673	1.754	4	0.288	3
16	43	78	16	2.692	1.322	19	0.401	19
17	9	83	17	2.721	1.309	20	0.417	20
18	31	88	18	2.759	1.455	18	0.386	18
19	27	93	19	2.785	1.667	9	0.315	9
20	7	98	20	2.887	1.535	14	0.378	16

Table 1: Flow Simulation Results. The *OOIP* ranking results are used to select the realizations to be processed for flow. The cumulative SOR and cumulative OP_{RATE} results and rank within the 20 realizations are shown.

VOLUMETRIC RANKING MEASURES					
NUMBER	REALIZATION	OIP		NET OIP	
		RANK (20)	*OOIP* (x10^6)	RANK	OIP_{NET} (x10^6)
1	50	1	2.298	2	2.159
2	59	2	2.415	8	2.304
3	88	3	2.436	4	2.173
4	2	4	2.455	7	2.249
5	37	5	2.478	1	2.113
6	3	6	2.520	5	2.193
7	56	7	2.540	6	2.238
8	60	8	2.568	11	2.38
9	23	9	2.579	10	2.374
10	40	10	2.596	9	2.366
11	64	11	2.623	13	2.44
12	95	12	2.637	3	2.164
13	86	13	2.646	14	2.487
14	81	14	2.663	15	2.511
15	42	15	2.673	12	2.413
16	43	16	2.692	16	2.557
17	9	17	2.721	18	2.586
18	31	18	2.759	17	2.573
19	27	19	2.785	19	2.657
20	7	20	2.887	20	2.714

Table 2: Volumetric Ranking Results. The volumetric ranking results for the 20 realizations selected for flow modeling.

STATISTICAL RANKING MEASURES							
NUMBER	REALIZATION	AVG POROSITY		AVG WATER SAT.		AVG PERMEABILITY	
		RANK	ϕ_{AVG}	RANK	S_{AVG}	RANK	k_{AVG}
1	50	7	0.313	1	0.329	11	1305.158
2	59	12	0.318	2	0.305	17	1367.274
3	88	4	0.307	4	0.267	5	1260.582
4	2	15	0.321	3	0.293	6	1263.947
5	37	1	0.297	9	0.231	4	1229.019
6	3	2	0.299	12	0.225	3	1179.330
7	56	6	0.311	8	0.249	2	1175.969
8	60	10	0.318	6	0.252	10	1296.960
9	23	13	0.318	7	0.250	14	1340.636
10	40	17	0.324	5	0.260	8	1281.549
11	64	5	0.311	16	0.218	12	1305.890
12	95	3	0.300	19	0.185	1	1045.448
13	86	9	0.318	10	0.229	16	1343.984
14	81	11	0.318	11	0.225	15	1342.857
15	42	14	0.319	13	0.225	9	1295.257
16	43	8	0.315	17	0.209	19	1485.717
17	9	19	0.324	14	0.223	13	1310.875
18	31	20	0.329	15	0.223	7	1280.988
19	27	16	0.323	18	0.201	18	1385.698
20	7	18	0.324	20	0.174	20	1487.685

Table 3: Statistical Ranking Results. The statistical ranking results for the 20 realizations selected for flow modeling.

GLOBAL CONNECTIVITY RANKING MEASURES					
NUMBER	REALIZATION	CONNECTED FRACTION		TORTUOSITY	
		RANK	F_{GC}	RANK	T
1	50	4	0.733	8	0.654
2	59	5	0.764	7	0.663
3	88	2	0.703	2	0.735
4	2	6	0.774	6	0.672
5	37	7	0.776	7	0.663
6	3	12	0.802	13	0.576
7	56	10	0.790	5	0.718
8	60	14	0.806	14	0.573
9	23	12	0.802	12	0.591
10	40	15	0.809	16	0.563
11	64	11	0.800	10	0.618
12	95	8	0.782	4	0.718
13	86	1	0.695	1	0.796
14	81	17	0.817	17	0.559
15	42	3	0.722	3	0.733
16	43	19	0.828	19	0.506
17	9	20	0.834	20	0.493
18	31	18	0.824	18	0.534
19	27	9	0.787	9	0.645
20	7	13	0.804	11	0.600

Table 4: Global Connectivity Ranking Results. The global connectivity ranking results for the 20 realizations selected for flow modeling.

LOCAL CONNECTIVITY RANKING MEASURES --- Y RADIUS = 1					
NUMBER	REALIZATION	CONNECTED FRACTION		CONNECTED THICKNESS	
		RANK	F_{LC}	RANK	*THK*
1	50	3	53.421	3	51.865
2	59	5	55.522	5	53.447
3	88	2	52.374	2	51.122
4	2	6	55.526	6	53.513
5	37	7	55.928	7	56.457
6	3	11	57.378	11	59.362
7	56	10	57.215	10	59.180
8	60	15	58.563	15	61.452
9	23	12	57.516	12	59.637
10	40	16	58.733	16	61.648
11	64	13	57.563	13	60.300
12	95	8	56.217	8	57.373
13	86	1	51.099	1	46.383
14	81	17	58.738	17	61.857
15	42	4	54.133	4	52.785
16	43	19	60.240	19	65.112
17	9	20	60.932	20	66.692
18	31	18	59.177	18	64.292
19	27	9	56.867	9	58.965
20	7	14	58.126	14	60.342

Table 5: Local Connectivity Ranking Results. The local connectivity ranking results for the 20 realizations selected for flow modeling.

RANKING PARAMETER CORRELATIONS									
PRODUCTION	VOLUMETRIC		STATISTICAL			GLOBAL CONN		LOCAL CONN	
	OOIP	OIP_{NET}	ϕ_{AVG}	S_{AVG}	k_{AVG}	F_{GC}	*T*	F_{LC}	*THK*
SOR	-0.521	-0.516	-0.324	0.400	-0.261	-0.907	0.891	-0.978	-0.964
O_{RATE}	0.432	0.508	0.388	-0.253	0.366	0.866	-0.846	0.902	0.888

Table 6: Correlation Results. The overall correlations between the static ranking measures and SAGD production performance.

LOCAL CONNECTIVITY CORRELATIONS												
PRODUCTION	Y RADIUS = 1		Y RADIUS = 2		Y RADIUS = 5		Y RADIUS = 10		Y RADIUS = 15		Y RADIUS = 20	
	F_{LC}	*THK*	F_{LC}	*THK*	F_{LC}	*THK*	F_{LC}	*THK*	F_{LC}	*THK*	F_{LC}	*THK*
SOR	-0.978	-0.964	-0.983	-0.972	-0.990	-0.979	-0.975	-0.962	-0.948	-0.934	-0.928	-0.914
O_{RATE}	0.902	0.888	0.906	0.898	0.910	0.898	0.902	0.878	0.882	0.848	0.832	0.818

Table 7: Local Connectivity Sensitivity. The correlation between the local connectivity ranking measure and SAGD production performance is optimized by considering different window sizes in the *Y* direction.

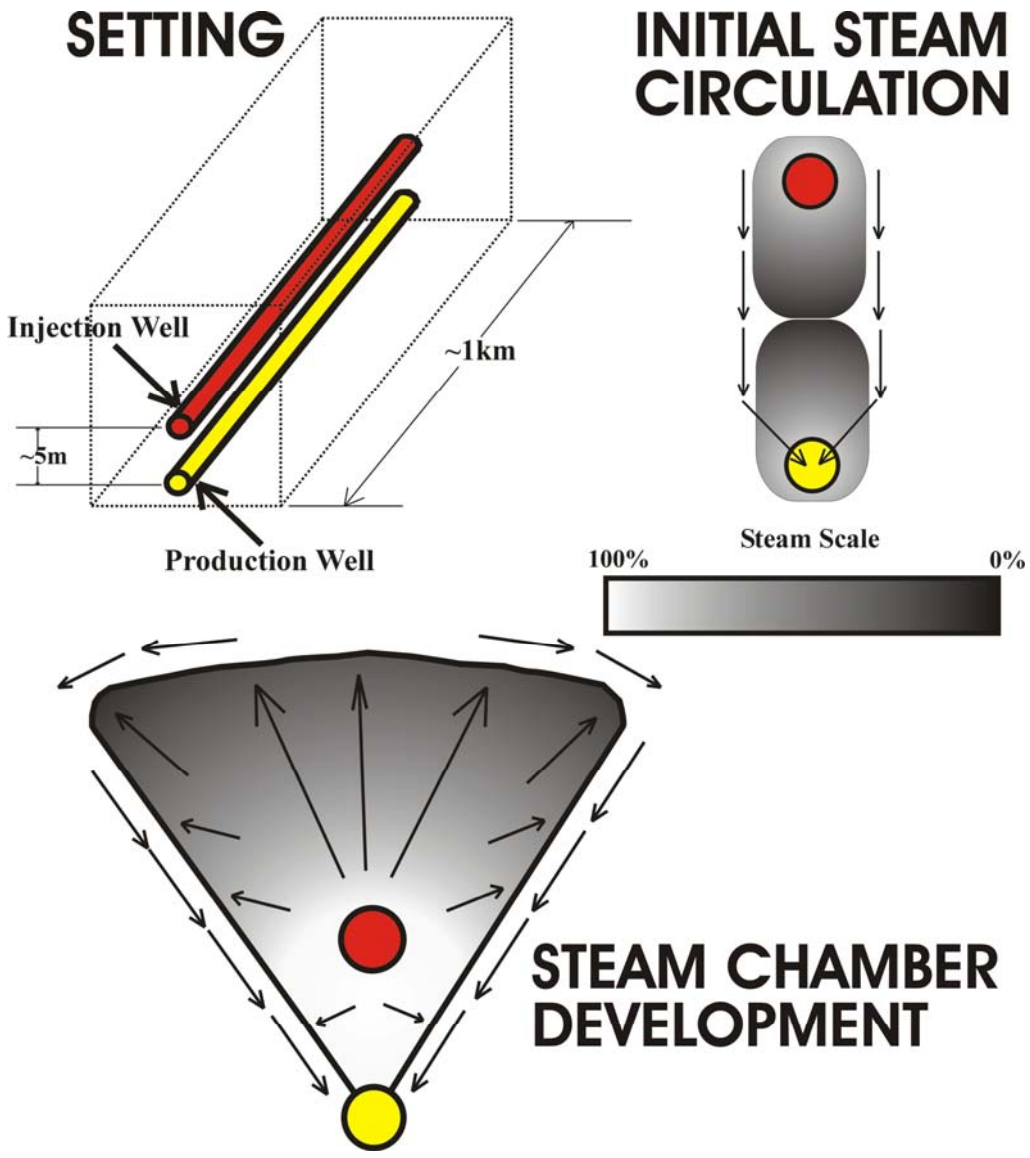

Figure 1: Steam Assisted Gravity Drainage (SAGD). The SAGD process is applied to horizontal well pairs (top left). Steam is first injected through both the injection and production well to initiate a steam chamber connecting the reservoir between wells. Steam circulation then continues in the injection well only forming a cone shaped steam chamber anchored at the production well (bottom). New bitumen is continually heated and drained along the outside of the steam chamber via gravity.

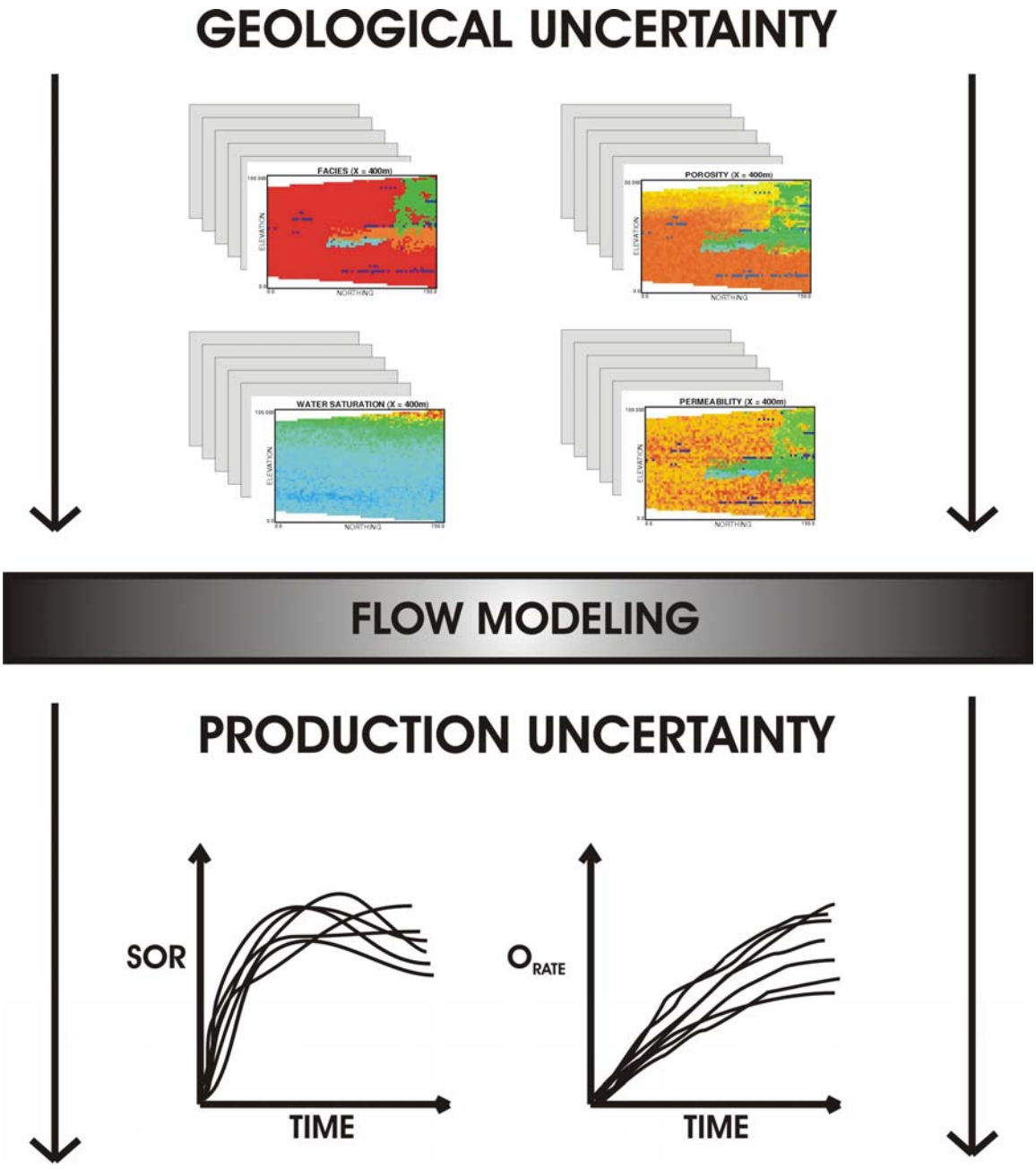

Figure 2: Uncertainty. Geostatistics is used to quantify geological uncertainty as the difference between multiple equally probable realizations of facies, porosity, water saturation, and permeability. Flow modeling provides the SAGD response (SOR and ORATE) for each realization. The difference between these responses is then a measure of production uncertainty.

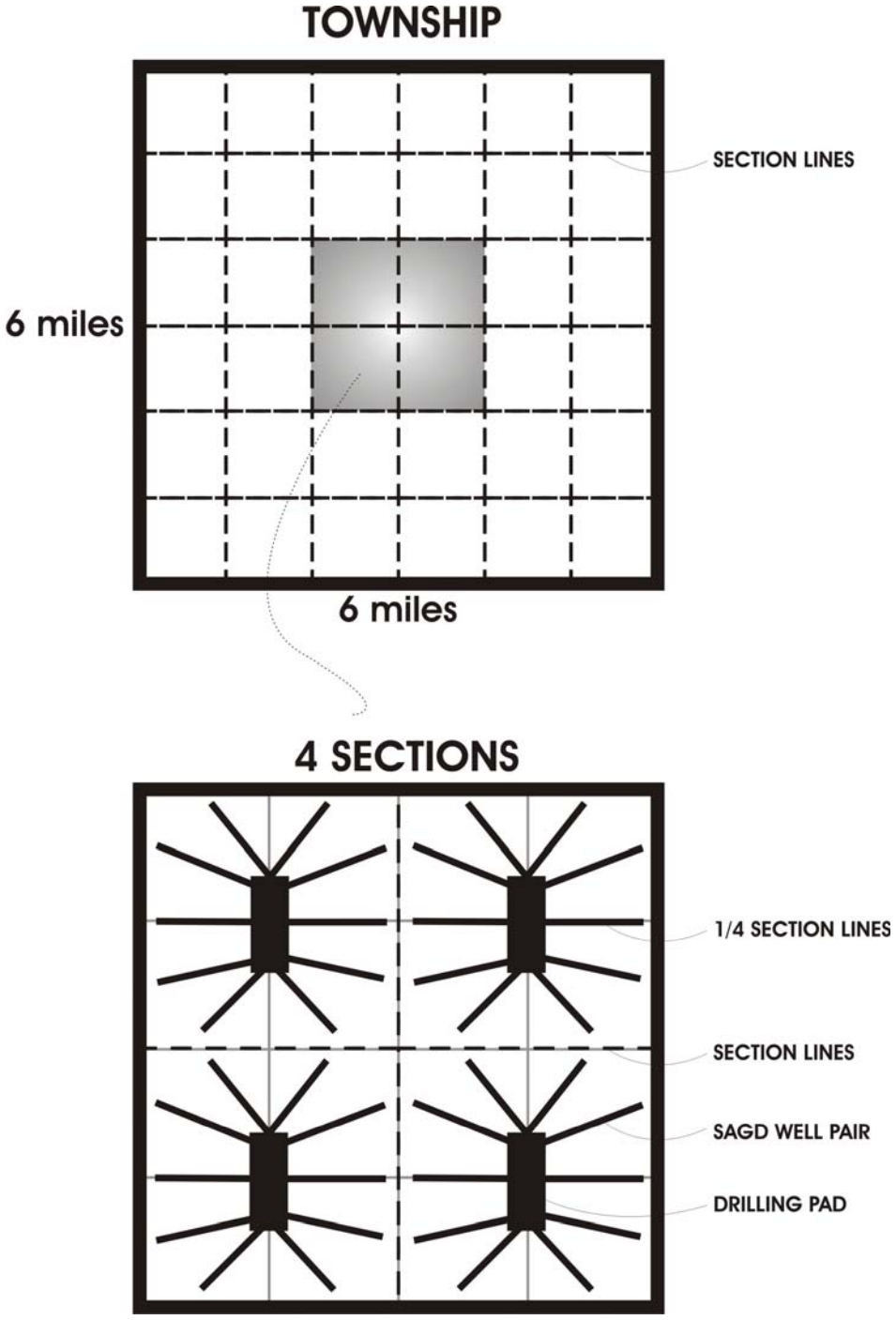

Figure 3: SAGD Example. A SAGD operation example showing 40 well pairs stemming from 4 drilling pads.

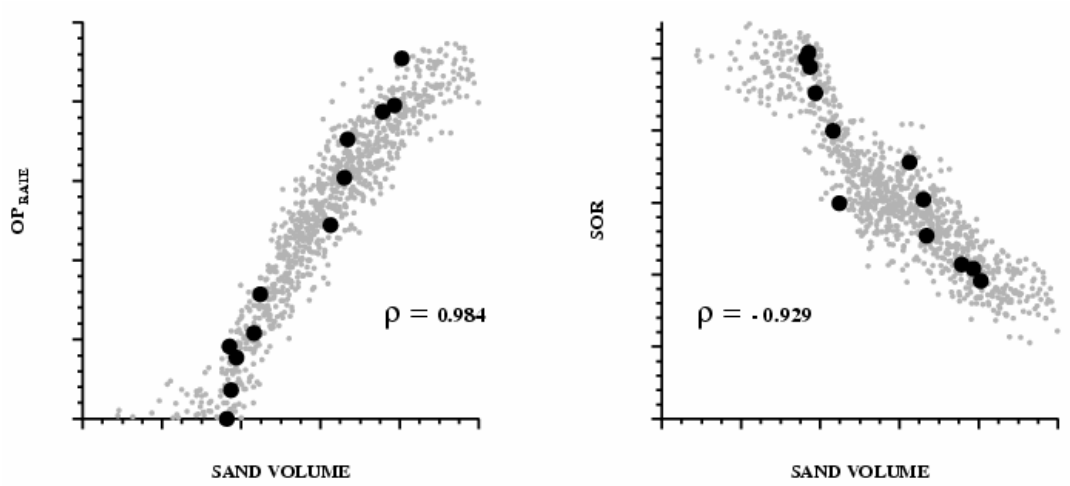

Figure 4: Ranking Example. Volume of sand is calculated on 100 realizations from 4 well pair drainage volumes. The low, medium, and high volume of sand realizations are then flow processed for OP_{RATE} and SOR (black dots). The calibration is then filled in (shaded dots) to infer the flow response for other drainage volumes.

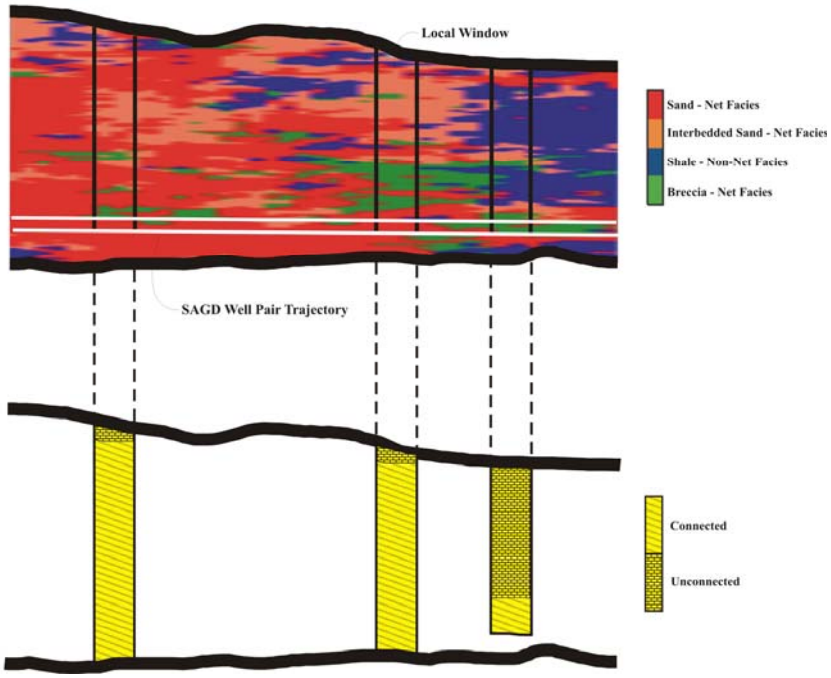

Figure 5: Local Connectivity. Only the net reservoir that is connected within local windows stemming from the well pair can be produced. The left 2 windows will produce the entire contained net reservoir; however, the steam chamber within the right window will not connect to upper net reservoir above the impermeable shale.

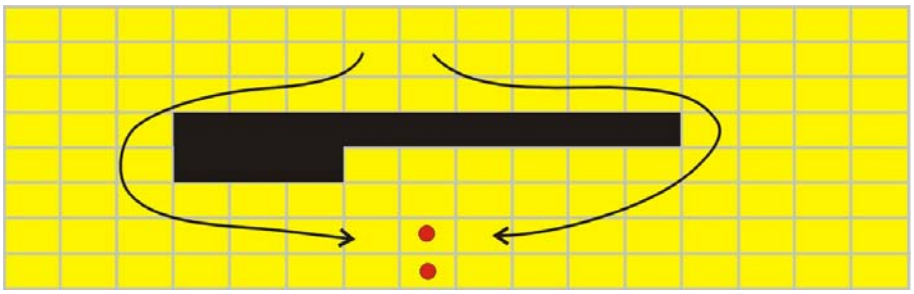

Figure 6: Global Connectivity Example. The entire net reservoir (yellow) is considered connected as a single geo-object even though the net reservoir above the impermeable shale (black) cannot be produced by the SAGD well pair (2 dots).

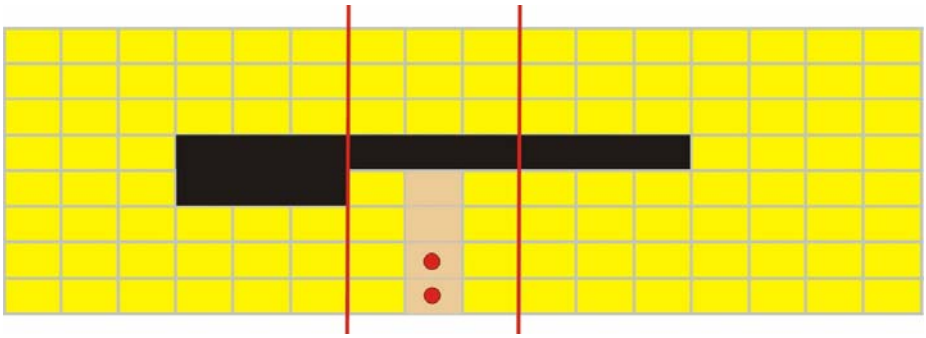

Figure 7: Local Connectivity (1). Connectivity is calculated for the middle column of cells within the window (vertical lines) tolerance. The string of 4 net reservoir cells immediately above and including the SAGD well pair are deemed connected.

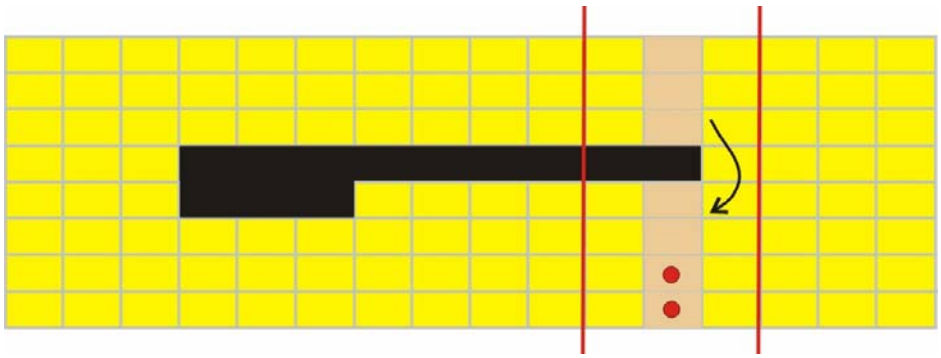

Figure 8: Connectivity (2). A particular stack of cells can be connected through the cells immediately above in the same column or the cells above and in adjacent columns within the window tolerance. Here, the full string of 7 net reservoir cells is deemed locally connected.

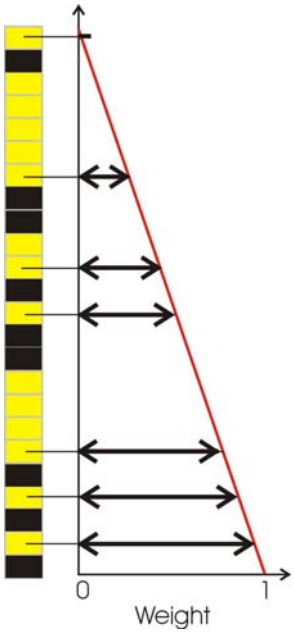

Figure 9: Local Connectivity Initialization. The elevation of the first cell considered in calculating connectivity within a particular stack of cells is important. The linear weighting function (red) is used to give higher weight to lower connected reservoir units and lower weight to higher connected reservoir units. The connectivity calculation begins within the lowest-thickest connected reservoir zone.

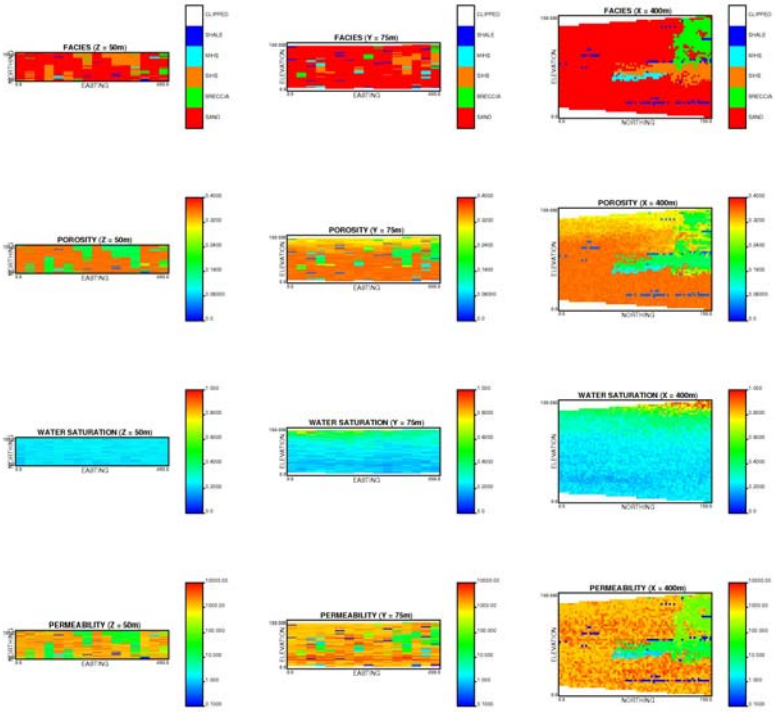

Figure 10: Reservoir Geology. A central *XY*, *XZ*, and *YZ* cross section through the 50th of 100 equally probable facies, porosity, water saturation, and permeability realizations.

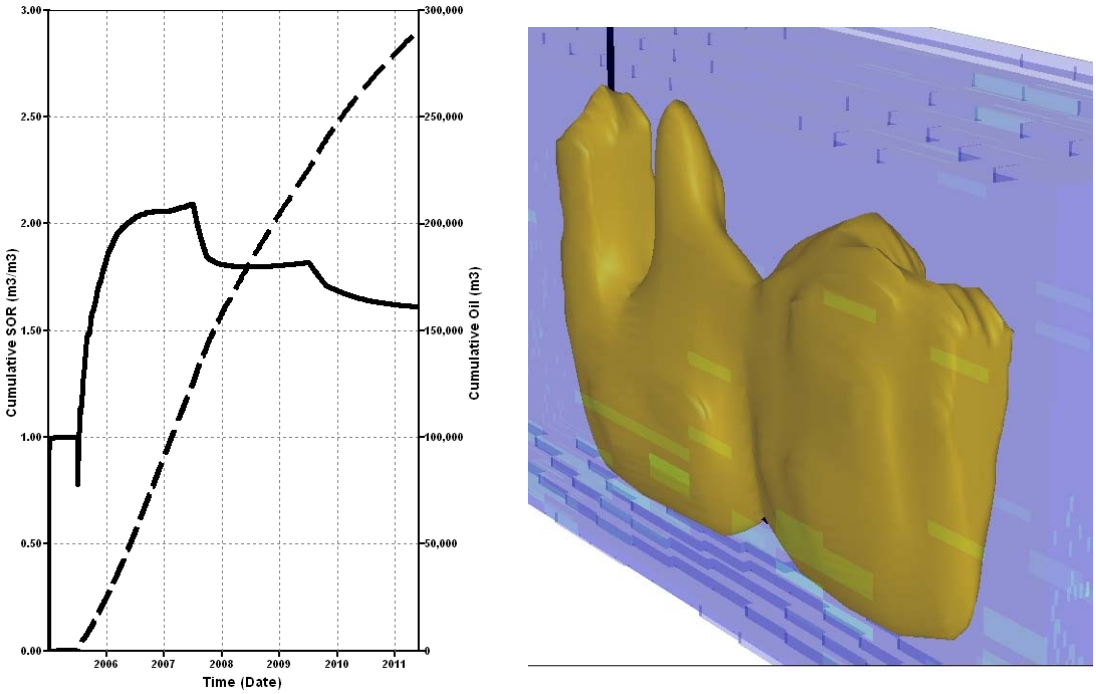

Figure 11: SAGD Production. The OP_{RATE} and SOR production profile for the middle ranked production response in terms of SOR.

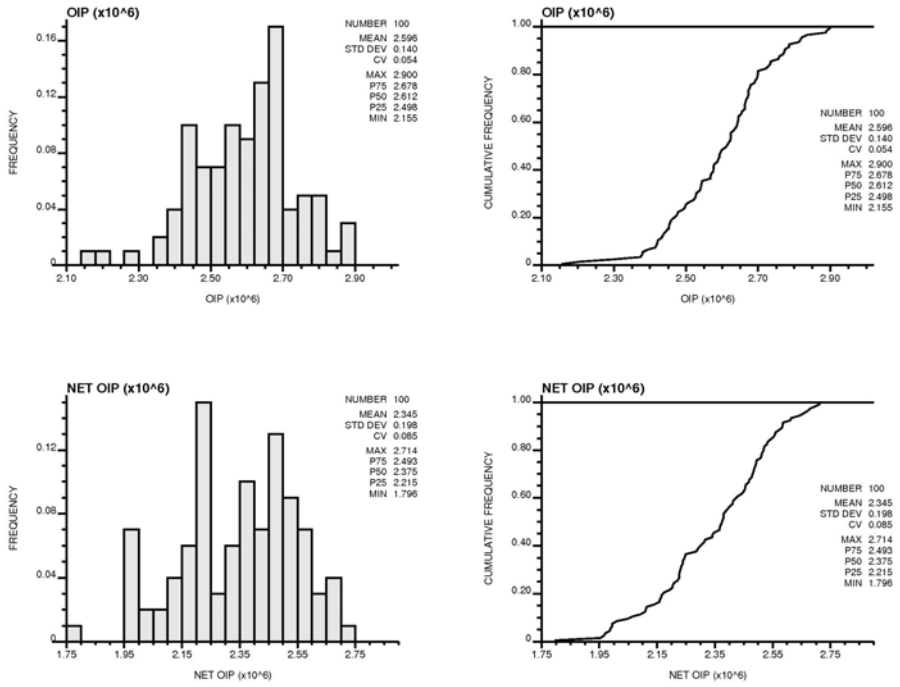

Figure 12: Volumetric Ranking Results. The volumetric ranking results for all 100 realizations.

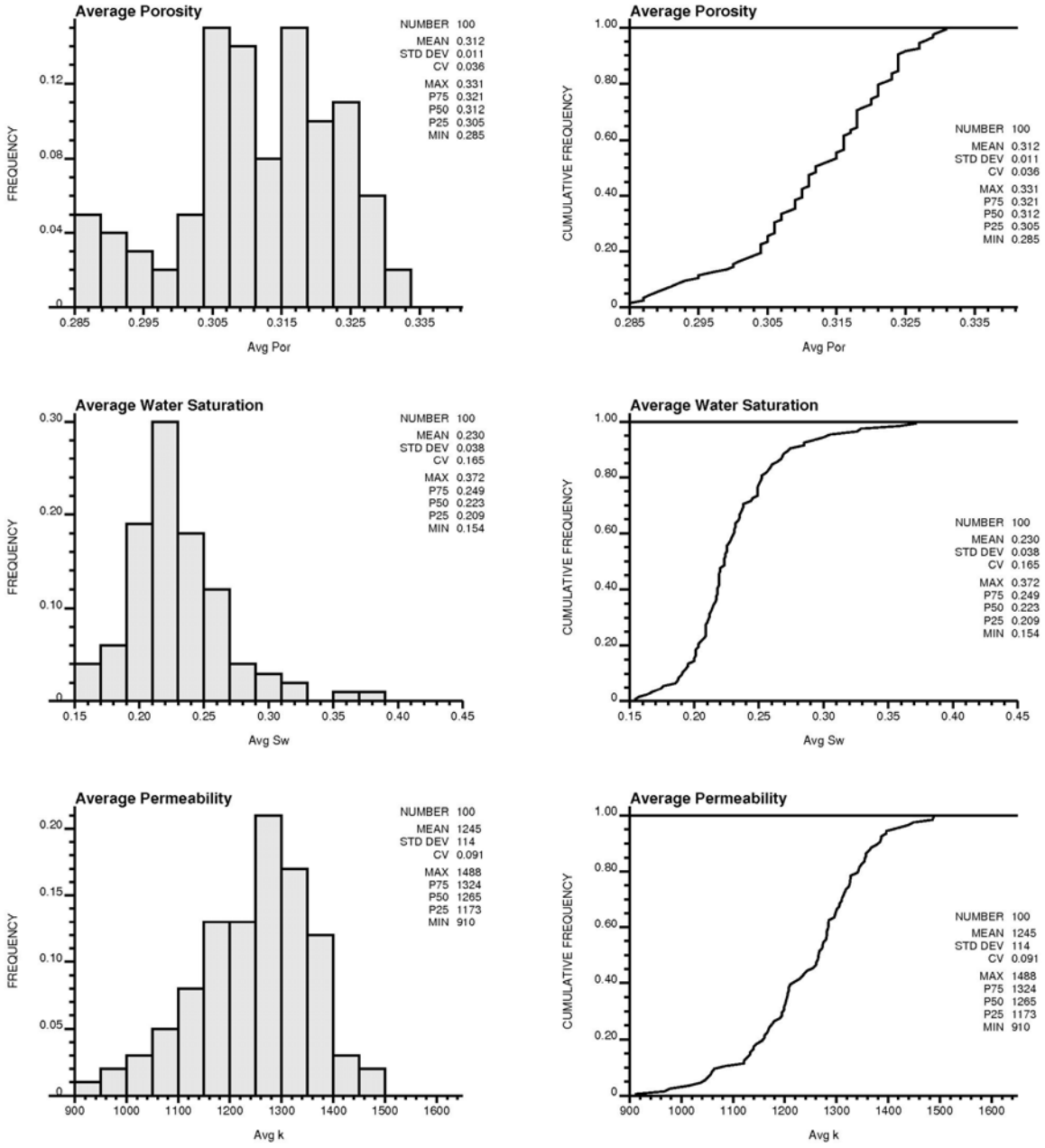

Figure 13: Statistical Ranking Results. The statistical ranking results for all 100 realizations.

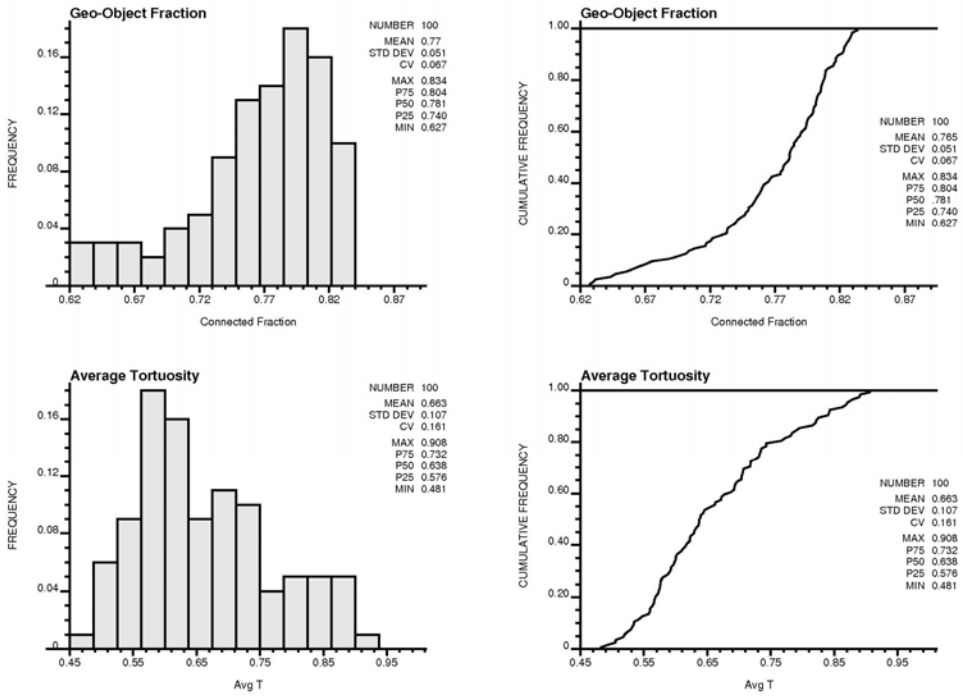

Figure 14: Global Connectivity Ranking Results. The global connectivity ranking results for all 100 realizations.

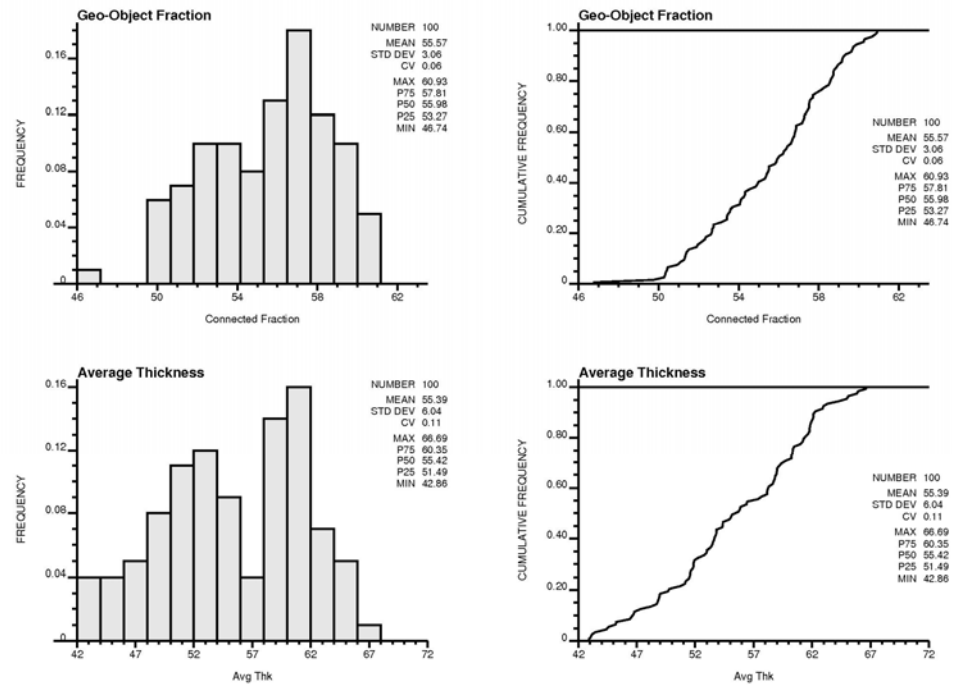

Figure 15: Local Connectivity Ranking Results. The local connectivity ranking results for all 100 realizations.